HEFAT2014 – paper # 1569903817
10th International Conference on Heat Transfer, Fluid Mechanics and Thermodynamics
14 – 16 July 2014
Orlando, Florida

CONCEPTUAL GLOBAL OPTIMAL BOUNDS FOR COP OF CASCADED-FLASHED R134a IRREVERSIBLE REFRIGERATION SYSTEM

Prof. Yousef M. Abdel-Rahim
Department of Mechanical Engineering
Faculty of Engineering
Assiut University, 71516, Egypt
(on Sabbatical leave to Univ. South Florida)
ymarahim@yahoo.com

Prof. Muhammad M. Rahman
Department of Mechanical Engineering
University of South Florida
4202 E. Fowler Avenue, ENB 118
Tampa, Florida 33620
mmrahman@usf.edu

ABSTRACT

Present study of the flash-mixed two-stage cascade R134a refrigeration system has considered the optimal COP cycle characteristics over whole ranges of all cycle controlling parameters, with consideration of pressure and thermal losses in all units and connecting lines of cycle. Application of Monte Carlo Method (MCM) has proved to be quite effective in optimizing cycle performance. COP, cooling power Q_{in}, total input power W_t and second law efficiency η_{II} are used as cycle performance parameters. Present COP and η_{II} results have been shown to compare well with other published results.

COP hyperbolically decreases with W_t. Higher COP values at lower W_t values exemplify the favorable use of this cycle in small-scale units. The study shows a parabolic relationship between COP and Q_{in}. Higher COP values at higher loads favor the use of this cycle for cooling purposes. Values of COP increase with η_{II}, justifyinging that reductions in cycle irreversibilities result in enhancement of COP. Systems having intermediate pressures that are about equal to geometric mean of terminal pressures as well as systems with about equal mass flow rates in upper and lower cycles result in optimum values of COP. This concludes that better systems have their units of comparable sizes.

MCM analysis shows that both evaporative temperature t_8 and inlet superheated temperatures to LP compressor t_{sup} have monotonic effects on conceptual optimal upper-enveloped COP bounds, with their optimum normalized values are both in the range 0.4 to 0.8 of their variation ranges of 265-284.4°K, 265.5-293.9°K respectively. COP is not sensitive to the cycle highest temperature T_4 as long as it is below about 332.5 °K, beyond which COP suffers very sharp decrease. This is in favor of using reasonable pressure ratio of HP compressor. Fitted equations are developed to relate upper bounds of COP with these three temperatures.

INTRODUCTION

With the phase-out of conventional refrigerants, heat pump and air conditioning systems are currently undergoing through significant redesigning efforts to improve their performance to fulfill the reliability requirements with environmentally-safe alternative refrigerants. Also, the increase of the energy prices and investment costs, have forced for more detailed thermo-economic analysis to optimize the performance of such systems and the redesign of cycle parameters to suit certain operating conditions. Such optimization studies are essential in reducing the environmental impact of energy utilization. Yet, the performance of commonly used heat pump units, as given in the literature, is highly influenced by the size and internal irreversibilities of the components composing those units.

Halimic et al. [1] compared the operating performance of three alternative refrigerants: R401A, R290 and R134a for use in a vapor compression refrigeration cycle. Their results indicated that the performance of R134a is very similar to that of R12, justifying the claim that it is a possible drop-in replacement for R12, but among the refrigerants tested, it gave the poorest performance. In their search for a drop-in replacement of R22, in heat pumps used for district heating in Sweden, Gabrielii and Vamling [2] reported that R134a is the only available alternative, resulting in a decrease of the heating capacity by about 35%. In their search for a better replacement among 2000 mixtures, their results showed that there are some

mixtures that can offer a higher heating capacity than R134a, but there is a decrease in COP. Cabello et al. [3] experimentally evaluated the vapor compression plant performance using R134a, R407C and R22 as working fluids, to study the influence of the evaporating pressure, condensing pressure and degree of superheat of the vapor on the cycle energetics. They concluded that the refrigerant mass flow rate was largely dependent on the suction conditions. Given the limited influence of the superheating and the rest of the variables considered, they showed that the mass flow rate was mainly governed by the compression ratio and the evaporating pressure and concluded that the mass flow rate has the most important influence on the refrigerating capacity. Brown et al. [4] evaluated COP for automotive air conditioning systems using CO_2 compared to those using R134a. They reported that, at speeds greater than 1000 rpm and ambient temperatures, the COP disparity was even greater. They indicated that the large entropy generation in the gas cooler in the CO_2 systems was the primary cause for their lower COP values. Grazzini and Rinaldi [5] developed a simulation program to search the maximum COP at given external fluid temperatures, mass flows, dimensions and temperature differences in the heat exchangers. For maximum COP, they numerically optimized the thermodynamic working conditions for given cooling power and inlet temperatures of cold and hot water streams. They confirmed the importance of the heat exchangers when high efficiency is required. Moreover, the greater COP corresponds to lower heat exchanger efficiency. In other words, the best working conditions of the system are different from those corresponding to optimized system components. They concluded that the phenomena involved in the cycle are not linear and there is a need to model the complete systems to find an optimum based on the thermodynamic functions of the external parameters and the need to search for a compromise.

Experimental evaluation of the internal heat exchanger influence on efficiency of a vapor compression refrigeration system working with R22, R134a and R407 conducted in [6] showed that internal or liquid-suction heat, to assure the entrance of liquid refrigerant to the expansion device, can have positive or negative influences on the plant overall efficiency, depending on the working fluid and the operating conditions. Their experimental results did not agree with the theoretical model when the pressure drops were neglected. Thermo-economic design optimization [7] of the tube-in-tube condenser in a vapor compression heat pump using three different refrigerants: R22, R134a and R410 concluded that the operating cost of the electric-driven heat pump depends on the overall exergy destruction rate in the system and thus efforts to improve plant efficiency become more and more advantageous. Selbas et al. [8] in their exergy-based thermo-economic optimization of subcooled and superheated vapor compression refrigeration R22, R134a, and R407C cycles have determined the optimum heat exchanger areas with the corresponding optimum subcooling and superheating temperatures using the Artificial Neural Network methodology. They concluded that system performance increases with subcooling and superheating operations. Valtz et al. [9] of the vapor–liquid equilibrium data for the R134a + dimethyl ether system at 293.18 to 358.15K temperatures and 0.4899 and 2.9442 MPa pressures stated that the isothermal P, x, y data can be well represented with the Redlich and Kwong equation of state. In their study, Arcaklıog et al. [10] have calculated second law efficiency and component irreversibility of a cooling system using R32, R125, R134a, R143A, R152A, R290 and R600A, based on constant cooling load with suction line heat exchanger. Their results showed that the 20/80 mass percentage of R32/R134a has provided the best efficiency level. Comparison of energetic performance of a variable-speed semi-hermetic reciprocating compressor using the R407C (R32/R125/R134a 23/25/52% in mass) conducted in [11] showed that it is possible to save about 12% electric energy consumption when an inverter control is employed instead of the on/off cycles thermostatic control. Szargut [12] in his work on component efficiencies of a vapor-compression heat pump in comparison with the Carnot heat pump showed that COP depends heavily on component efficiencies.

Ust [13] performed performance analysis and optimization of irreversible air refrigeration models having finite-rate of heat transfer, heat leakage and internal irreversibilities based on ecological coefficient of performance (ECOP) criterion and analytically derived corresponding optimal isentropic temperature ratio, optimal entropy generation rate and the optimal cooling. He indicated that the performance parameters at the maximum ECOP and maximum COP are the same. Jung et al. [14] investigated the performance of the cascade multi-functional heat pump and experimentally compared the results with that of the single-stage multi-functional heat pump. They optimized the heating load varying the refrigerant charge, and showed that the cascade system gave higher and more stable heating capacity than the single-stage unit. Wu et al. [15] designed a cascade heat pump with a thermal storage tank using R404A/R134a, and measured the transient behavior and dynamic performance of the heat pump system. Park et al. [16] studied the fundamental performance of the steady-state model of a cascade heat pump system equipped with a dynamic model of a storage tank under a limited control logic aimed at a specific degree of superheat based on experimental results. They found that the system power increases, while its COP diminishes as the storage tank is filled with hot water. They indicated that when ambient temperature gets colder, the average system COP decreases whereas the operation time and the power consumption of a heat pump increase, and the system operation was dependent on the balance of the two cycles using compressors frequency and refrigerant charge amount. They concluded that successive research is needed to cope with various situations, such as one for maximum COP and maximum heat capacity.

Recently, The R134a-R410A cascade cycle has been introduced into heat pump water heaters [17]. The cascade system enables a heavy load of heat pump water heaters to be distributed to two different refrigeration cycles which can operate with a fair performance. Some studies have been carried out to analyze the performance of cascade heat pump water heaters and to optimize them. Park et al. [18] conducted experiments to obtain the optimal intermediate temperature of the cascade heat pump water heater. They found the optimal temperature which made the system achieve maximum efficiency and established correlations to find out the temperature. Wu et al. [19] designed a cascade heat pump water heater with a phase change material for thermal energy storage application. They discussed the difference between the cascade system and the single stage system. Also, they clarified the contribution of a phase change material by comparing the energy performance with and without water tanks. Jung et al. [20] compared the cascade heat pump water heater and a single-stage heat pump by experiments. They found that the cascade system showed more stable operation and higher water outlet temperature. Abdel-Rahim and Sharif [21] presented and discussed the optimal allocation of heat exchanger inventory for maximum COP and exergitic performance of a two-stage vapor compression cycle.

The above review shows that there have been a significant number of researches done to study of R134a vapor compression refrigeration systems for various applications. Yet, there still some more work needed for performance enhancement of the conventional R134a cycle provided that some trade-off optimization techniques are utilized to cover possible operating ranges of system parameters. The present paper considers the two-stage refrigeration system with flash and mixing chambers with the R134a as the refrigerant. The conventional thermodynamic first law and second law cycle COP calculations is augmented by the Monte Carlo method to incrementally cover the effects of the controlling cycle parameters varied over their whole operating ranges. This method is a trade-off technique for the design of a system composing units to fulfill the objective of cycle optimization, a method that has proved to be very effective. Other traditional optimization methods will not lead to the required objectives due to the complex thermodynamic properties relationships of the refrigerant and the thermodynamic governing nonlinear equations for different units of the system.

The present paper seeks the optimal COP of the two-stage cascade R134a refrigeration system with flash chamber over the full operating ranges of all cycle controlling parameters. The COP, total heat in, total work and second law efficiency are used as cycle performance parameters. The following sections give the cycle description and the necessary analysis.

CYCLE DESCRIPTION

The irreversible R134a two-stage cycle with flash and mixing chambers along with the presumed pressure and thermal losses is depicted in Fig. 1. The refrigerant leaves the condenser as a saturated liquid and is throttled to a flash chamber operating at P_6. The refrigerant leaving the low-pressure compressor (LP) at state 2 is routed to a mixing chamber where it is mixed with the vapor leaving the flash chamber and then compressed to the condenser pressure by the high-pressure compressor (HP). The liquid from the flash chamber is throttled to the inlet to the evaporator at pressure P_8. The compressors have isentropic efficiencies η_A, η_B. Losses in pressures and enthalpies are considered in this study. The refrigeration heat load is carried by the cycle in process 8-1. States 5 and 7 are assumed saturated liquid, while state 3 is assumed saturated vapor. The study considered the inlet to the LP compressor to be between saturation and 10 K degrees superheated. The ratio of the flow rates in the HP cycle (denoted m_A with assumed value of 0.1 kg/s) and the LP cycle (denoted m_B) depend on values of the low, intermediate and high operating pressures of the cascade cycle.

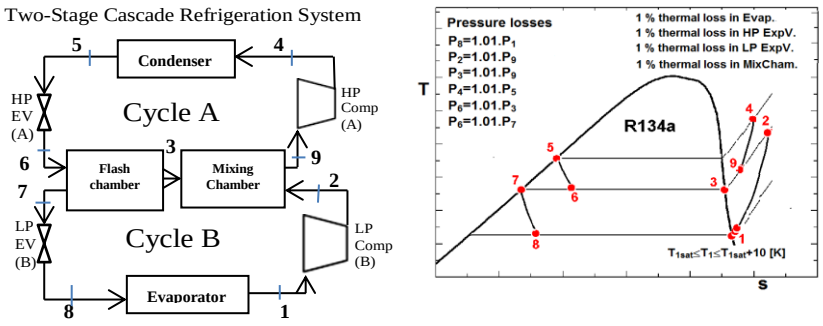

Fig.1 Representation and the T-s diagram of the two stage R134A compression cycle with flash and mixing chambers.

ANALYSIS

The thermodynamic analysis of the 8 composing units of the Flashed-Mixed-Cascaded system, shown in Fig. 1, has been applied and programmed on EES. This analysis is based on 1st and 2nd laws of thermodynamics [22] as well as the thermodynamic properties of the refrigerant R134a. Appendix A summarizes the simulation equations. For exergy analysis, the dead state conditions are assumed as P_0=101.3252 kPa and T_0=298 K. The analysis is done in two versions:

(i) Controlled selection of the cycle controlling parameters.

For the sake of comparisons of present analysis with published works, a set of calculations have been conducted with controlled selections of some of the cycle controlling parameters at certain levels, while the values of the other parameters are kept constant. The results of this controlled selection is discussed in the following discussion section and compared with other published results.

(ii) Random selection of the cycle controlling parameters: The Monte Carlo Method (MCM), as discussed in [23], is used in this part. The MCM necessitates that complete cycle calculations are done based on random selections of the cycle controlling parameters. The MCM then screens out the cycle performance results to determine the conceptual global optimal bounds for the COP of the cycle. The MCM depends on the declaration of two requirements: (i) The declaration of suitable wide variation ranges for the cycle controlling parameters to serve as the sampling domain for the random selection to help the comprehensive investigation of the effects of the parameters on the cycle performance; and (ii) The declaration of suitable realistic criteria to reject the unsuitable cycle performance results.

To fulfill the first requirement of variation range declaration, and to simulate realistic wide operation, the analysis considers three types of irreversibility losses: (a) isentropic LP and HP compressors efficiencies (ranging from 70% and 95%), (b) pressure drops in all system flow lines (ranging from 0% to 10% of their upper value in each respected line) and (c) thermal energy losses in condenser, expansion valves, mixing chamber and evaporator (ranging from 0% to 10% of their upper values in each respected unit). These irreversibility losses serve three folds: (i) to encounter the system operation away from the design point, like the case of starting and stopping periods and the case of changes in the thermal load during operation, (ii) to exemplify the effects of many degradation factors such as: deterioration of the system units due to aging, the leakage in compressors, the emulsion of the lubricating oil with the refrigerant, … etc. and (iii) to reach a conceptual COP optimal evaluation through the global survey of the effects of cycle controlling parameters over their realistic variation ranges. This COP optimal global random MCM search method surpasses the conventional rate differentiation method which is mainly devoted to localized optimal values. The realistic variation ranges of the controlling parameters of the cycle used in the study are shown in Table (B1) in Appendix B.

To fulfill the second requirement, the rejection criterions include many factors such as rejection of results if in any of the following cases: first law efficiency η_I, second law efficiency η_{II} or Carnot efficiency η_{car} values ≥ 1.0, pressure ratios P_2 / P_1 and $P_4 / P_9 \leq 1$, negative values that contradict layout of the cycle (such as differences in entropies s_4-s_9, s_6-s_5, s_8-s_7), … etc.

The methodology of the MCM can be summarized as follows:
(i) Choose the minimum number of the controlling parameters of the cycle that is sufficient to completely solve the cycle from the following list of parameters:

$$(P_1, P_2, P_4, P_9, T_1, T_4, T_5, T_9, V_1, V_2, V_4, V_9, m_B).$$

(ii) For each of the chosen cycle parameters in step (i), select a random value from its respected variation range. The variation ranges for the controlling parameters used in the study are given in Table (B1) in Appendix B.
(iii) Conduct a complete set of solution for the performance of the cycle.
(iv) Repeat the above 3 steps for 10,000 times for other random choices of the controlling parameters to cover their whole variation ranges.
(v) Based on the above-discussed rejection criterion, reject any complete cycle calculations that have any unrealistic results of any of the performance parameters of the cycle.
(vi) Tabulate the acceptable results to perform the conceptual COP optimization search. Table (B2) in Appendix B gives the resulting acceptable ranges for the cycle performance values. The performance values included in the study are:

$$(COP, Q_{in}, W_t, I_t, m_{AB}, \eta_{II}, w_{cA}/v_9, w_{cB}/v_1, P_1.P_4/P_2^2, w_{AB}, v_{12}, v_{94}, vol_{cap})$$

RESULTS AND DISCUSSION

Results under controlled selection of parameters: The effects of the highest cycle pressure (P_4) and intermediate cycle pressure (P_6) on the cycle performance are displayed in Fig.2 (a), (b) and (c). In Fig. 2(a), the value of COP is high for higher values of P_6 and lower values of P_4. COP value monotonically drops with the increase in P_4. The second law efficiency η_{II} is high for both higher P_6 and lower P_4 values As expected, the closer these pressures to each other, the better this efficiency is. The total input work to compressors increase almost linearly with the high cycle pressure P_4 but decrease with the increase of P_6. Fig.2 (b) shows the effect of P_6 on COP, W_t and η_{II} at 3 different values of P_4.The parabolic variations of both COP and Wt with P_6 signify the existence of upper values of these performance parameters in the range 500 – 750 kPa for P_6. Again, as expected, the input power decreases with the increase of both P_6 and P_4. The effect of P_6 on cycle temperatures and exegy values at different locations around the upper cycle are shown in Fig. 2(c) at a value of the highest cycle pressure P_4 = 1200 kPa. The most affected states by the intermediate pressure P_6 are states 6 and 9, where they exhibit sharp increase with the increase of this pressure. Opposing to this behavior, states 4 and 5 show an almost independent behavior in regards to the effect of P_6 , where their values show an almost constant behavior. The highest levels of exergy values are for states 4, 5 and 6 respectively, while state 3 (state between the mixing chamber and flash chamber) shows the lowest level in terms of exergy values for the whole range of variation of P_6 . The value of this exergy loss of the mixing chamber decreases with the increase in P_6 and will vanish when the intermediate and highest cycle pressures are equal. In this figure, when the intermediate and higher pressures of the cycle are equal (i.e.: $P_4 = P_6$ = 1200 kPa) state 4 and 9 coincide (meaning the HP

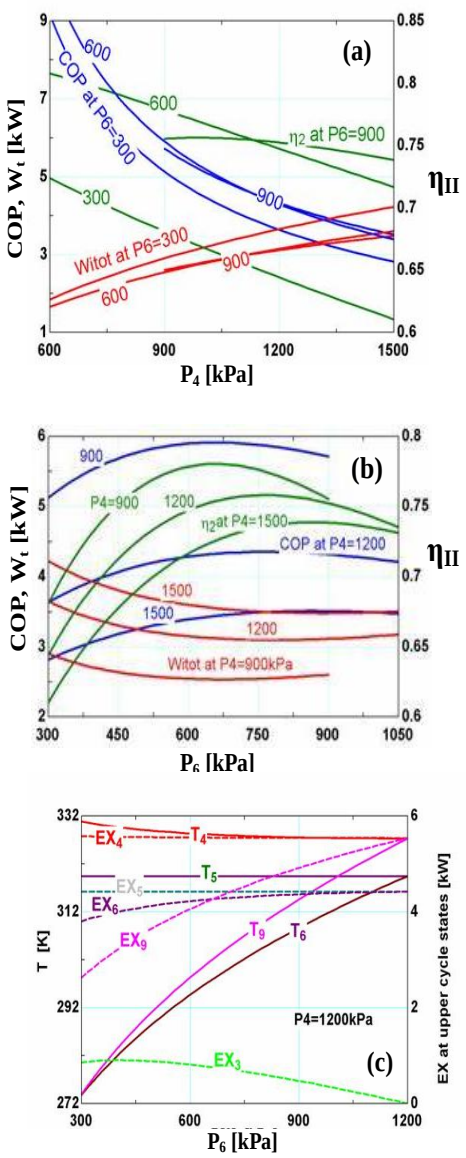

Fig. 2. Effect of higher (P_4) and intermediate (P_6) cycle pressures on cycle performance.

compressor is cancelled) and states 5 and 6 coincide (meaning the HP EV is cancelled), resulting in only a single stage compression system with neither a mixing chamber nor a flash chamber.

Comparison with published results of Ref. [24]: For the sake of comparisons of present analysis with published works, a set of calculations have been conducted in the present study with controlled selections of some of the cycle controlling parameters at certain levels, while the values of the other parameters are kept constant. Although the present curves were not exactly calculated at same conditions of those of the references used in comparisons, yet the general trends of variations should exemplify and justify the comparison. Fig. 3 shows the values of COP and η_{II} as dependent on the

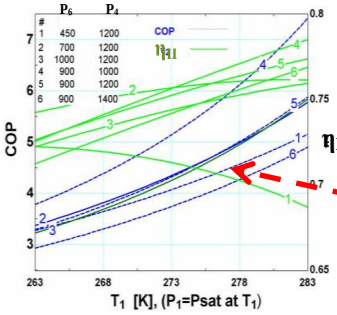

Fig.3. Effect of evaporative temperature T_1 on cycle performance at different 6 levels of intermediate (P_6) and higher (P_4) pressures of the cycle.

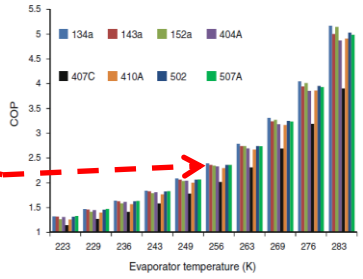

Fig. 8 of Ref. [24] Evaporative temperature Versus COP.

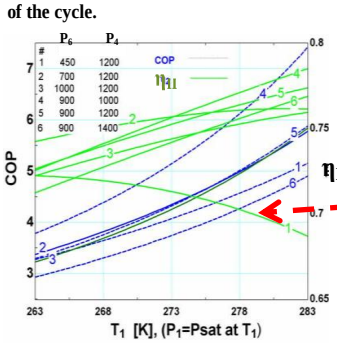

Fig.3. Effect of evaporative temperature T_1 on cycle performance at different 6 levels of intermediate (P_6) and higher (P_4) pressures of the cycle.

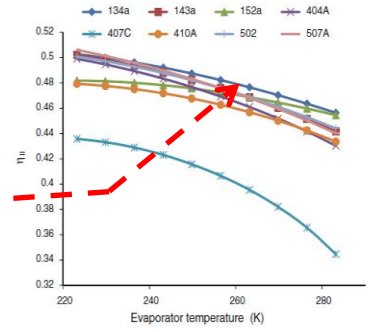

Fig. 9 of Ref. [24] Evaporative temperature Versus exergitic efficiency.

evaporative temperature T_1 at 6 levels of values of the cycle intermediate P_6 and highest P_4 cycle pressures. Also, the displayed Fig. 8 of Reference [24] shows the variation of COP with the evaporative temperature for 8 different refrigerants including R134a. At values of P_4 = 1200 kPa and P_6 = 450 kPa, in Fig. 3, the variation of COP shows a parabolic increase with T_1, which agrees well with the displayed behavior COP in Fig. 8 of Ref [24] for R134a. Differences in COP values shown in the curves between those of the present study and those of Ref. [24] are due to: (i) differences between the systems considered in these studied; and (ii) differences of the conditions under which these two results have been calculated.

Fig. 9 of Ref. [24] displays the effect of evaporative temperature on the second law efficiency η_{II} for 8 refrigerants including R134a. The behavior of the efficiency for R134a in this figure shows a monotonic decrease with the evaporation temperature which agrees well with that shown in Fig. 3 of the results of present study at P_4 = 1200 kPa and P_6 = 450 kPa . Again, differences in η_{II} values shown in the curves of the present study and those of Ref. [24] are due same two reasons mentioned above.

Appendix C shows another comparison with other published data of Ref. [25].

Results of MCM application: The application of the MCM, as outlined in the above analysis, results in the scattered data

points displayed in Figs. 4 (a), (b), (c) relating COP as dependent on total power input to the cycle; W_t, total heat input to evaporator; Q_{in} and total irreversibility losses of the cycle; I_t and in Figs. 5 (a), (b), (c) relating COP as dependent on second law efficiency of the cycle; η_{II}, the intermediate to terminal pressures ratio of the cycle; $(P_1.P_4/P_6^2)$ and the upper to lower mass flow rates; m_{AB} respectively. In these figures, each data point represents one complete set of cycle calculations. The reason for this scattered behavior in these figures, because each shown point represents a set of calculations where the values of the cycle controlling parameters are not chosen in a controlled manner, but rather in a random manner. This means that Fig. 4(a) shows the ultimate and only effect of W_t on COP regardless of the values of the other cycle controlling parameters, because these parameters have been surveyed all-over their variation ranges. As well, Fig. 4(b) and Fig. 4(c) show the ultimate and only effects of cycle Q_{in} and I_t on COP respectively regardless of the values of the other cycle controlling parameters. The red dashed shapes in these figures envelope the optimum values of COP with regards to the designated independent parameter irrespective of any value of the other controlling parameters.

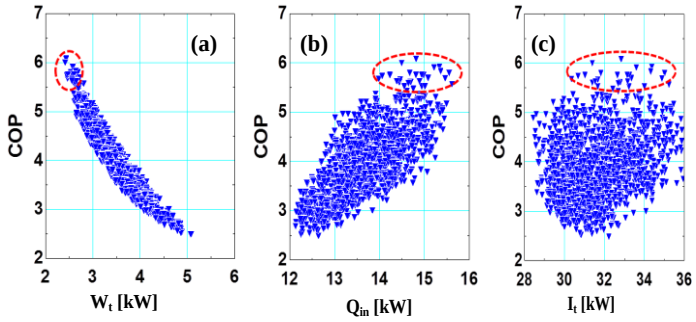

Fig.4. Variations of COP with (a) power input W_t, (b) thermal cooling load Q_{in} and (c) total cycle irreversibility losses I_t.
(Note: Data points in these figures are results of random selection of all other cycle controlling parameters except the designated independent parameter).

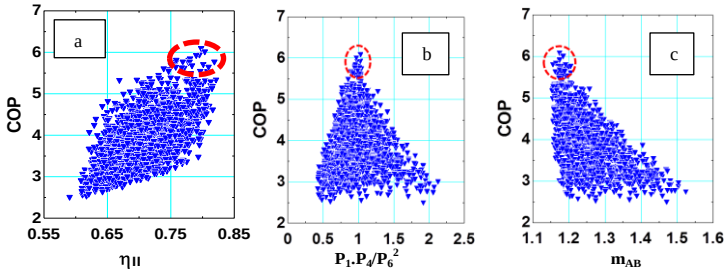

Fig.5. Variations of COP with (a) second law efficiency η_{II}, (b) terminal to intermediate pressure ratio $(P_1.P_4/P_6^2)$ and (c) mass flow ratio m_{AB}.
(Note: Data points in these figures are results of random selection of all other cycle controlling parameters except the designated independent parameter).

Displayed relationships in Figs. 4 (a), (b) and (c) show high COP values for less cycle total power, high cooling load and moderate irreversibility losses. The general trend in Fig. 4(a) shows a hyperbolic decreasing relationship of COP with the input power W_t . The narrow scatter of the points in this figure exemplifies a very good dependency of COP on cycle power. The high value of COP at low input power exemplifies the favorable use of this cycle in small scale units. Although the scatter in Fig. 4 (b) is not as narrow as in Fig. 4 (a), yet it shows a generally parabolic increasing relationship between COP and Q_{in}. In this figure, the higher the cooling loads the higher the COP of the cycle. This result supports the use of this system in cooling purposes. Figure 4 (c) shows that the COP dependency on I_t is weak, due to the large scatter of the data points relating them.

Figures 5 (a), (b), (c) show the ultimate and only effects on COP of second law efficiency of the cycle; η_{II}, the intermediate to terminal pressures ratio of the cycle; $(P_1.P_4/P_6^2)$ and the upper to lower mass flow rates; m_{AB} respectively. Again, the red dashed shapes in these figures locate the maximum values of COP in each figure. As expected, Fig.5 (a) shows that the value of COP increases with the increase in second law efficiency, meaning that the benefits in reducing the cycle irreversibilities have been used in enhancing COP. COP is nearly optimum around pressure ratio of about 1, as in Fig.5 (b), a case which is supported by the well-known result in thermodynamics in optimizing total work of two-stage compression process. As the ratio of the mass flow rates between the upper and lower cycles approaches a value of 1, as shown in Fig. 5(c), the COP approaches its optimum value. Both Figs. 5(b) and (c) show a very strong dependency of COP on both the intermediate to terminal pressures ratio; $(P_1.P_4/P_6^2)$ and the upper to lower mass flow rates; m_{AB}.

Optimal Bounds for COP: For the sake of conceptual optimal upper bounds of COP, under all possible variations of the cycle controlling parameters, the results presented above, as scattered data points in the past two figures, have been enveloped from above along the whole variation range of the independent parameter, as shown in Fig. 6.

For sake of uniformity, these envelopes, which encompass the highest COP values along the whole domain of each of the shown controlling parameters, have been plotted against normalized values of the independent parameters; i.e.: normalized initial temperature $t_1=(T_1-T_{1min})/(T_{1max}-T_{1min})$. T_{1max} and T_{1min} are the maximum and minimum temperatures that are screened by MCM to be the boundary of the accepted temperature range for feasible cycle operation. The figure gives the values of these temperatures. Upper COP envelopes with respect to normalized inlet temperature to the LP compressor; t_1,the degree of superheat; t_{sup} and the highest cycle temperature; t_4 together with the MCM scattered data results are shown in the figure.

Monotonic effects of both t_1 and t_{sup} on COP give optimum values for these two parameters to be in the range 0.4 to 0.8, where the COP is in its higher range. Outside this range, the COP suffers a decrease in its value. The figure shows the

value of COP is not sensitive to the highest cycle temperature t_4 as long as it is below about 0.6. Above this value, COP suffers very sharp decrease with the increase in t_4. This means that any high power input to the HP is not in the favor of the cycle operation and leads to a low value of COP, a case which is supported by the results shown and discussed in Fig. 4 (a) relating COP to total power input to the cycle.

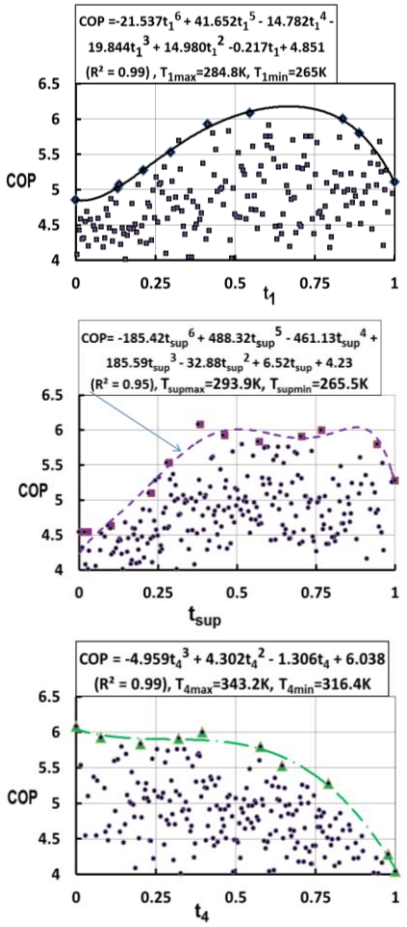

Fig.6. Upper bound of COP with respect to normalized values of initial temperature t_1, degree of superheat t_{sup} and maximum cycle temperature t_4.

CONCLUSIONS

Present study simulates the two-stage cascaded-flashed R134a AC system including pressure and thermal losses in all units and connecting lines of the cycle. Results of cycle analysis for both COP and second law efficiency η_{II} have been shown to compare well with other published results. The study discussed the optimum levels for COP values as dependent on cycle controlling parameters. High COP values are obtained for less cycle total input power due to the hyperbolic decreasing relationship of COP with input power W_t . This exemplifies the favorable use of this cycle in small-scale units. The parabolic relationship between COP and the cooling load Q_{in} shows high COP values for high load, favoring the use of this cycle for cooling purposes.

Values of COP increase with the increase in η_{II}, meaning that benefits in reducing cycle irreversibilities have been used in enhancing COP. COP is nearly optimum around cycle intermediate to terminal pressures ratio of about 1, a case that is supported by thermodynamics in optimizing total work of two-stage compression. COP approaches its optimum value at unity ratio of upper to lower cycles mass flow rates, favoring a sized-balanced upper and lower cycles.

Conceptual optimal upper-enveloped COP bounds show monotonic effects of both t_1 and t_{sup} on COP. Optimum values for these two normalized temperatures are in the range 0.4 to 0.8, where the COP is in its highest range. COP is not sensitive to the highest cycle temperature t_4 as long as its normalized value is below about 0.6. Above this value, COP suffers very sharp decrease. This means that increasing the power input to the HP is not in favor of the cycle operation and leads to a low value of COP. Fitted equations for these COP upper bounds with these temperatures and pressures are developed.

REFERENCES

[1] E. Halimic, D. Ross, B. Agnew, A. Anderson and I. Potts. A comparison of the operating performance of alternative refrigerants. Applied Thermal Eng. 23 (2003) 1441–1451.

[2] C. Gabrielii and L. Vamling. Drop-in replacement of R22 in heat pumps used for district heating – influence of equipment and property limitations. Int. J. Refrig. 24 (2001) 660-675.

[3] R. Cabello, E. Torrella, and J. Navarro-Esbri. Experimental evaluation of a vapor compression plant performance using R134a, R407C and R22 as working fluids. Applied Thermal Eng. 24(2004)1905-1917.

[4] J. S. Brown, S. F. Yana-Motta and P. A. Domanski. Comparative analysis of an automotive air conditioning systems operating with CO2 and R134a, Int. J. Refrig. 25 (2002) 19–32.

[5] G. Grazzini and R. Rinaldi. Thermodynamic optimal design of heat exchangers for an irreversible refrigerator. Int. J. Therm. Sci. (2001) 40, 173–180.

[6] J. Navarro-Esbrı, R. Cabelloa and E. Torrella. Experimental evaluation of the internal heat exchanger influence on a vapor compression plant energy efficiency working with R22, R134a and R407C. Energy 30 (2005) 621–636.

[7] M. Dentice d'Accadia and L. Vanoli. Thermoeconomic optimization of the condenser in a vapor compression heat pump. Int. J. Refrig. 27 (2004) 433–441.

[8] R. Selbas, O. Kızılkan and A. Sencan. Thermoeconomic optimization of subcooled and superheated vapor compression refrigeration cycle. Energy 31 (2006) 2108–2128.

[9] A. Valtz, L. Gicquel, C. Coquelet and D. Richon. Vapor–liquid equilibrium data for the 1,1,1,2 tetrafluoroethane (R134a) + dimethyl ether (DME) system at temperatures from 293.18 to 358.15K and pressures up to about 3MPa. Fluid Phase Equilibria 230 (2005) 184–191.

[10] E. Arcaklıog, A. Cavusoglu and A. Erisen. An algorithmic approach towards finding better refrigerant substitutes of CFCs in terms of the second law of thermodynamics. Energy Conversion and Management 46 (2005) 1595–1611.

[11] C. Aprea, R. Mastrullo, C. Renno and G. P. Vanoli. An evaluation of R22 substitutes performances regulating continuously the compressor refrigeration capacity. Applied Thermal Eng. 24 (2004) 127–139.

[12] J. Szargut. Component efficiencies of a vapor-compression heat pump. Technical University of Silesia, Institute of Thermal Tech. Konarskiego 22, 44-101 Gliwice, Poland, August 2001.

[13] Y. Ust. Performance comparison between a single-stage and a cascade multi-functional heat pump for both air heating and hot water supply. Applied Thermal Eng. 29 (2009) 47–55.

[14] H. W. Jung, H. Kang, W. J. Yoon and Y. Kim. Performance comparison between a single-stage and a cascade multi-functional heat pump for both air heating and hot water supply. Int. J. Refrig. 36 (2013) 1431-1441.

[15] J. Wu, Z. Yang, Q. Wu and Y. Zhu. Transient behavior and dynamic performance of cascade heat pump water heater with thermal storage system. Appl. Energy 91, (2012) 187-196.

[16] H. Park, D. H. Kim and M. S. Kim. Performance investigation of a cascade heat pump water heating system with a quasi-steady state analysis. Energy 63 (2013) 283-294.

[17] N. Park, H. Park, S. Jung, J. Shin, B. Chung and D. Kang. On the optimal inverter operation of air-source heat pump water heater with thermal energy storage. In: Proceedings of the 8th JSME-KSME thermal and fluids Eng. Conf. 2012.

[18] H. Park, D. H. Kim and M. S. Kim. An experimental study on the optimal intermediate temperature of a cascade refrigeration system with R134a and R410A. Proceed., 6th Asian conf. on Refrig. and air-conditioning 2012.

[19] J. Wu, Z. Yang, Q. Wu and Y. Zhu. Transient behavior and dynamic performance of cascade heat pump water heater with thermal storage system. Appl. Energy 2012;91(1):187-96.

[20] H. W. Jung, H. Kang, W.J. Yoon and Y. Kim. Performance comparison between a single stage and a cascade multi-functional heat pump for both air heating and hot water supply. Int. J. Refrig. 2013; 36(5):1431-41.

[21] Y. M. Abdel-Rahim and S. A. Sharif. Optimal allocation of heat exchanger inventory for maximum COP and exergitic performance of a two-stage vapor compression cycle. ASME Summer Heat Transfer Conf., 14-19, July 2013, Minneapolis, MN USA.

[22] M. Moran and H. Shapiro. Fundamentals of engineering thermodynamics. John Wiley and Sons, 5th , 2006. England.

[23] Y. M. Abdel-Rahim. Monte-Carlo optimization of two-stage cascade R134a refrigeration system with flash chamber. Proceedings of Design Eng. Tech. Conf. & Computers and Information in Eng. Conf., IDETC/CIE, paper #DETC2008-49063, August 3-6, 2008, NY, USA.

[24] V. S. Reddy, N. L. Panwar and S. C. Kaushik. Exergitic analysis of a vapour compression refrigeration system with R134a, R1431, R152a, R404A, R407C, R410A, R502 and R507A. Clean Techn Environ Policy (2012) 14:47-53. DOI 10.1007/s10098-011-0374-0.

[25] J. Navarro-Esbri, J. M. Mendoza-Miranda, A. Mota-Babiloni, A. Barragan-Cervera and J. M. Belman-Flores. Experimental analysis of R1234yf as a drop-in replacement for R134a in a vapour compression system. Int. J. Refrig., 36(2013)870-880.

APPENDIX A: SIMULATION EQUATIONS OF THE CYCLE

HP Compressor "A" (Mass flow rate: $m_A = 0.1$kg/s)
Pressure drop in line 3-9: $P_3 = 1.01*P_9$;
Isentropic enthalpy at state 4s (h_{4s}), where: $P_{4s} = P_4$, $s_{4s} = s_9$
Energy balance on isentropic compressor: $h_9 + w_{As} = h_{4s}$
Definition of compressor isentropic efficiency: $w_A = w_{As}/\eta_{cA}$
Energy balance on real adiabatic compressor: $h_9 + w_{cA} = h_4$
Total power of HP compressor: $W_A = m_A*w_A$

Condenser (State 5 is saturated liquid)
Pressure drop in line 4-5: $1.01*P_5=P_4$
energy balance on condenser: $h_4=q_{out}+h_5$
Total heat losses in condenser: $Q_{out} = m_A*q_{out}$

Throttle Valve A
Energy balance with thermal losses: $h_6*1.01=h_5$

Flash Chamber (State 7 is saturated liquid)
Mass balance: $m_B = (1-x_6) * m_A$;
Pressure drop in line 6-7: $1.01*P_7= P_6$
Energy balance: $Q_{637}=m_A*h_6 - m_B*h_7 -(m_A - m_B)*h_3$

Mixing Chamber (State 3 is saturated vapor)
Energy balance: $(m_A - m_B)* h_3+ m_B * h_2=(x_6* m_A + m_B)* h_9*1.01$;
Pressure drop in line 3-6: $1.01* P_3 = P_6$
$T_{sup}= T_1+DT_1$
Pressure drop in line 2-9: $P_2= P_9*1.01$

LP Compressor "B"
Energy balance on isentropic compressor: $h_1+ w_{Bs}= h_{2s}$
Definition of compressor isentropic efficiency: $w_B = w_{Bs}/\eta_{cB}$
Energy balance on real compressor: $h_1+ w_B= h_2$
Total LP compressor power: $W_B=m_B*w_B$

Throttle Valve B

Energy balance with thermal losses: $h_8*1.01=h_7$

Evaporator

Pressure drop in line 8-1: $P_8= P_1*1.01$
Energy balance on evaporator with losses: $1.01*q_{in} + h_8= h_1$
Total heat input (Thermal load): $Q_{in}=m_B*q_{in}$

Cycle Statistics

Total input power: $W_t = W_A + W_B$;
Definition of coefficient of performance: $COP=Q_{in}/W_t$
Dead state conditions: $T_0=298\ ^oK$, $P_0=101.325$ kPa,

Second law efficiency: $\eta_{II}=((1-T_0/T_5)*Q_{out}-(1-T_0/T_1)*Q_{in})/W_t$
Volumetric cooling capacity: $VolCoolCap=(q_{in}/v_1)*\eta_{idvol}$
Ideal vol. efficiency: $\eta_{idvol} = 1-(v_2/(v_1- v_2)*((P_2/P_1)^{(1/1.106)}-1))$
Specific exergy at state "i": $\varepsilon_i = h_i-h_0-T_0*(s_1-s_0)$, i=1, 2, .., 9
Exergy difference in process i-j = $(\varepsilon_j - \varepsilon_i)$*mass flow rate
Irreversibility loss in process i-j = $T_0*(s_j - s_i)$*mas flow rate
Total cycle irreversibility losses $I_t= I_{12} + I_{81} + I_{78} + I_{56} + I_{94} + I_{45} + I_{376} + I_{923}$

APPENDIX B: VARIATION RANGES OF CYCLE CONTROLLING AND PERFORMANCE PARAMETERS

Table C1. Practical variation ranges of cycle controlling parameters, (Temperatures in ^oK , Pressures in kPa, m_A=0.1kg/s):

Parameter	P_1	P_2	P_4	P_6	P_9	T_1	T_2	T_3	T_4	T_5	T_9	η_{cA} , η_{cB}	m_B (kg/s)
Min.	**215.9**	**372.8**	**900.1**	**376.5**	**369.1**	**265**	**285.4**	**280**	**316.4**	**308.3**	**281.2**	0.7	**0.066**
Max.	**438.4**	**905.9**	**1500**	**914.9**	**896.9**	**284.8**	**329.7**	**308.9**	**348.1**	**327.9**	**322.9**	**0.95**	**0.087**
Std. Dev.	**52.2**	**117.6**	**154.9**	**118.8**	**116.4**	**4.9**	**7.9**	**6.3**	**6.1**	**4.9**	**7.7**	**0.07**	**0.004**

Table C2. Resulting variation ranges of the performance parameters of the cycle:

Parameter	W_{cA}	W_{cB}	Q_{in}	W_{in}	Q_{out}	COP	η_{II}	W_{cA}/V_9	W_{cB}/V_1	$\frac{(W_{cA}/V_9)}{(W_{cB}/V_1)}$
Units	kW							kJ/m^3		
Min.	**1.13**	**0.84**	**12.13**	**2.41**	**15.29**	**2.49**	**0.59**	322.99	134.87	1.06
Max.	**3.88**	**3.25**	**15.61**	**5.08**	**18.71**	**6.08**	**0.82**	779.04	463.72	4.82
Std. Dev.	**0.47**	**0.45**	**0.72**	**0.48**	**0.62**	**0.66**	**0.05**	87.34	63.99	0.59

APPENDIX C: COMPARISON OF PRESENT COP RESULTS WITH PUBLISHED RESULTS OF REF. [25]

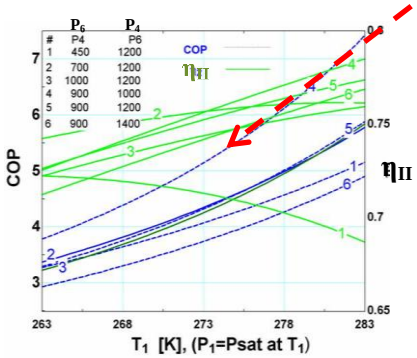

Fig.3. Effect of evaporative temperature T_1 on cycle performance at different 6 levels of intermediate (P_6) and higher (P_4) pressures of the cycle.

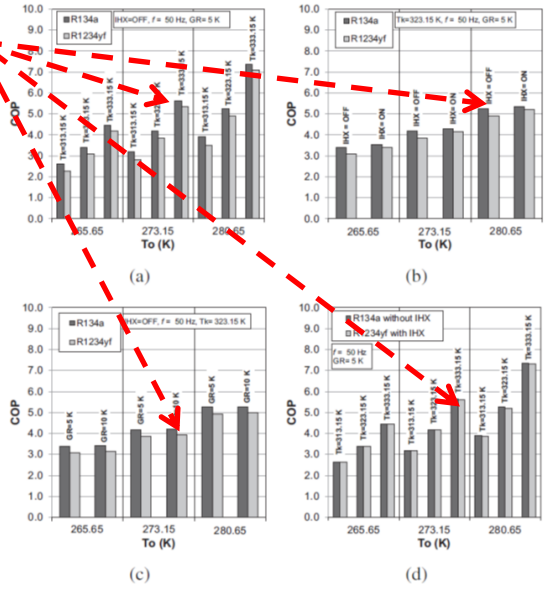

Fig. 6 of Ref. [25] Theoretical COP variation versus evaporation temperature T_0: (a) varying condensing temperature, (b) with and without IHX, (c) varying superheating degree, (d) comparing R1234yf with IHX and R134a without IHX.